Aerospace Science and Technology 39 (2014) 22–30

Contents lists available at ScienceDirect

Aerospace Science and Technology

www.elsevier.com/locate/aescte

Investigation of transonic bi-convex corner flows

Kung-Ming Chung [a,*], Po-Hsiung Chang [b,1], Keh-Chin Chang [b,2], Frank K. Lu [c,3]

[a] Aerospace Science and Technology Research Centre, National Cheng Kung University, Tainan, Taiwan
[b] Department of Aeronautics and Astronautics, National Cheng Kung University, Tainan, Taiwan
[c] Aerodynamic Research Center, Department of Mechanical and Aerospace Engineering, The University of Texas at Arlington, Arlington, TX, USA

ARTICLE INFO

Article history:
Received 20 May 2014
Received in revised form 14 July 2014
Accepted 27 August 2014
Available online 2 September 2014

Keywords:
Bi-convex corner
Expansion flow
Shock-induced
Boundary-layer separation

ABSTRACT

Experiments were performed to investigate a transonic, turbulent boundary layer over a bi-convex corner. The total turning angle η ranged from 10 deg to 17 deg. In subsonic expansion flows, the presence of a bi-convex corner results in a decrease in local peak Mach number M_{peak} and the amplitude of peak surface pressure fluctuations $(\sigma_p/p_w)_{max}$. There is a delay in transition from subsonic to transonic expansion flows. A dual expansion is observed in transonic expansion flows. Shock structure, boundary-layer separation and $(\sigma_p/p_w)_{max}$ were dependent on freestream Mach number M, first turning angle η_1 and η. The length of the first corner L_1 also plays an important role. An increase in L_1 results in less flow expansion, while a decrease in the amplitude of $(\sigma_p/p_w)_{max}$ is associated with a shorter L_1.

1. Introduction

Trailing-edge devices of a wing evolve from plain to Fowler flaps with single, double, and even triple slots. Previous studies [12,21,22] indicated that active modification of control surfaces (variable wing camber control) can potentially play a role in performance optimization for large transport aircraft. A simplified deflected control surface comprises a convex-corner (upper surface) and a concave corner (lower surface). For compressible convex-corner flows, Ruban et al. [18] demonstrated that a viscous-inviscid interaction whereby the displacement thickness near the corner is affected by the overlapping region that lies between the viscous sublayer and the main part of the boundary layer. The viscous sublayer exhibits high sensitivity to pressure variations. A small pressure rise would lead to thickening of flow filaments. Further, when the flow is accelerated to sonic speed, the sonic line originates from the corner apex and separates the subsonic and supersonic regions. There is an additional acceleration in the Prandtl–Meyer expansion downstream [19]. In turbulent flows, there are upstream expansion and downstream compression near the corner apex. At higher M and η, the flow switches from a subsonic expansion flow to a transonic one [3]. The boundary layer would be separated with unsteadiness of the interaction being characterized by local peak pressure fluctuations due to adverse pressure gradient and shock excursion phenomenon [4,5].

In the present study, surface pressure measurements and surface oil flow visualization were conducted to investigate the flow properties of transonic bi-convex corner flows ($M = 0.64$–0.89), corresponding to a trailing-edge device with double slots with the overall convex angle η ranging from 10- to 17-deg. In addition, a study of a double ramp flow by Gaisbauer et al. [10] indicated that the length of the first ramp is an important parameter in shock-induced, boundary-layer separation. Therefore, the effect of L_1 on flow development was also examined. Before discussing the results of the present study, details of the experiment are outlined next.

2. Experimental setup

2.1. Transonic wind tunnel and test models

Experiments were conducted in the blowdown transonic wind tunnel at the Aerospace Science and Technology Research Center/National Cheng Kung University (ASTRC/NCKU), as shown in Fig. 1. Major components of the facility include compressors, air dryers, a cooling water system, three air storage tanks and the tunnel. The constant-area test section, assembled with solid sidewalls, and perforated top and bottom walls with a fixed porosity of 6%, is 600×600 mm^2 and 1500 mm in length. The perforated walls with 60 deg inclined holes serve to eliminate or minimize the wall interference of the test section. A rotary perforated sleeve

* Corresponding author. Research fellow and Director. Tel.: +886 62392811x210; fax: +886 62391915.
E-mail addresses: kmchung@mail.ncku.edu.tw (K.-M. Chung), kiby716@gmail.com (P.-H. Chang), kcchang@mail.ncku.edu.tw (K.-C. Chang), franklu@uta.edu (F.K. Lu).
1 Graduate research associate.
2 Professor.
3 Professor.

http://dx.doi.org/10.1016/j.ast.2014.08.012
1270-9638/

Nomenclature

L_1	length of the first convex corner	x_i^*	region of separated boundary layer, x_i/δ
M	freestream Mach number	β	similarity parameter, $M^2\eta/\sqrt{1-M^2}$
M_{peak}	local peak Mach number	η	convex-corner angle
p_∞, p_w	mean surface static pressure	η_1	first turning angle
q	freestream dynamic pressure	δ	incoming boundary-layer thickness
x	coordinate along the surface of the corner .... cm	σ_p	standard deviation of surface pressure
x^*	normalized streamwise distance, x/δ		

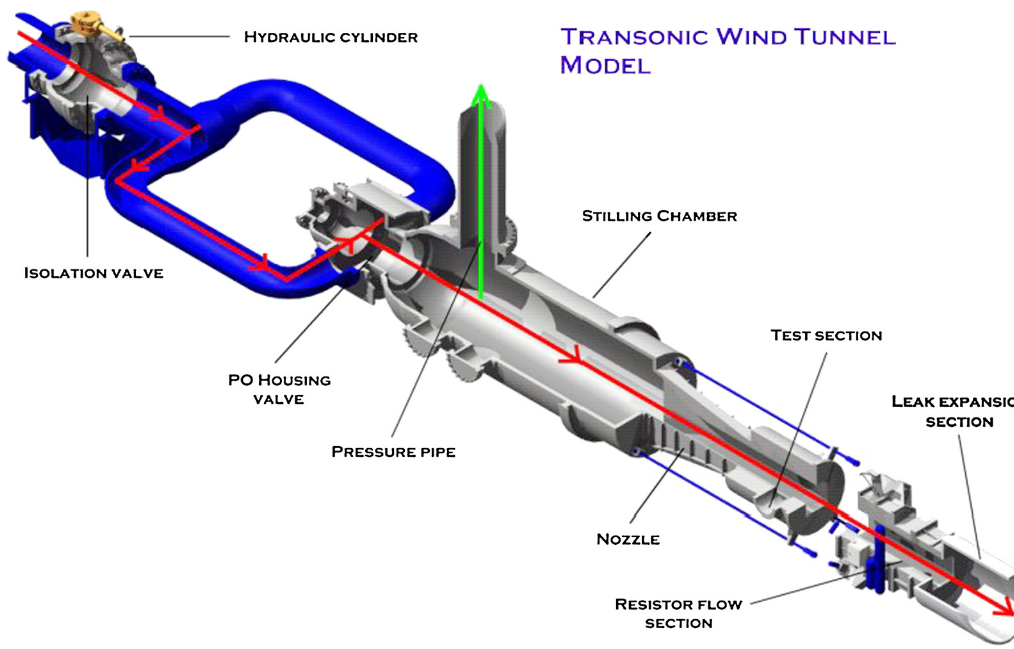

Fig. 1. ASTRC/NCKU transonic wind tunnel.

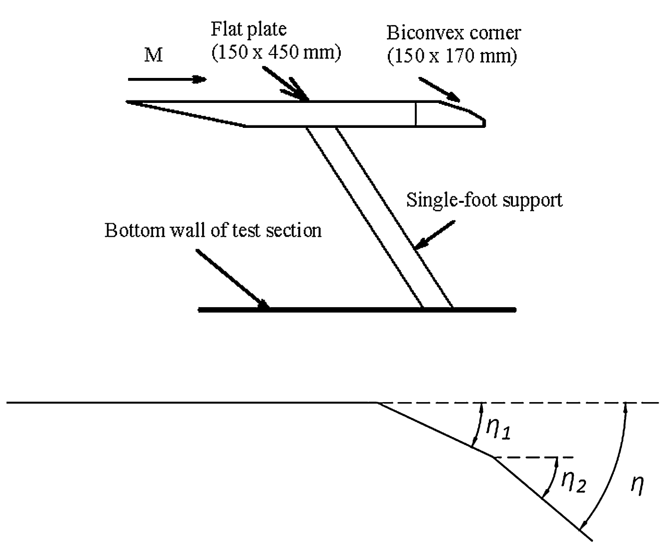

Fig. 2. Test configuration.

valve monitored the stagnation pressure level, which was $p_o = 172 \pm 0.5$ kPa in the present study. The stagnation temperature T_0 was the ambient value. Downstream of the test section, the hinged choke flaps were rotated onto the stream to provide choke control of the test section. The freestream Mach number was 0.64, 0.70, 0.83 and 0.89 ± 0.01, and the unit Reynolds number ranged from 20.1 to 24.1 million per meter.

The test model, which was supported by a single sting, comprised a flat plate that was 150 mm wide × 450 mm long and an interchangeable instrumentation plate with a bi-convex corner (150×170 mm^2), as shown in Fig. 2. The model surface was 30 cm from the bottom floor of the test section (or in the center). The first convex corner was located 500 mm from the 4 deg sharp leading edge of the flat plate for a naturally developed, turbulent boundary layer. The normalized velocity profiles for the undisturbed boundary layer at 25 mm upstream of the sharp convex corner appeared to be full ($n \approx 7$–11 for the velocity power law), and the boundary-layer thickness δ was estimated to be approximately 7 mm [4]. The values of η were 10-, 13-, 15- and 17-deg, in which the first convex-corner angle η_1 was 5- or 7-deg, as shown in Table 1. For surface pressure measurements, one row of 19 pressure taps (spacing of 6 mm center to center) along the centerline of each instrumentation plate was drilled perpendicularly to the test surface. Further, the typical L_1 distance was 12 mm ($\approx 1.7\delta$, Case A). For the cases of $\eta = 13$- and 15-deg, $L_1 = 12$ and 24 mm ($\approx 3.4\delta$, Case B). Two side fences of ($13.5 \times 4.5 \times 0.5$ cm^3) were also installed at both sides of the instrumentation plate to prevent crossflow.

2.2. Instrumentation and data acquisition system

For dynamic pressure measurements, flush-mounted Kulite pressure transducers (XCS-093-25A, B screen) with a nominal outer diameter of 2.36 mm and a pressure-sensitive element of 0.97 mm in diameter were used. The natural frequency is 200 kHz, as quoted by the manufacturer. Note that the perforated screen of